mathematics

MDPI

Article

Lyapunov-Based Two-Degree-of-Freedom Model Reference Adaptive Control of Axial-Piston Pump

Tsonyo Slavov [1], Alexander Mitov [2,*] and Jordan Kralev [1]

[1] Department of Systems and Control, Technical University of Sofia, Kliment Ohridski 8 Boulevard, 1000 Sofia, Bulgaria; ts_slavov@tu-sofia.bg (T.S.); jkralev@tu-sofia.bg (J.K.)
[2] Department of Hydroaerodynamics and Hydraulic Machines, Technical University of Sofia, Kliment Ohridski 8 Boulevard, 1000 Sofia, Bulgaria
* Correspondence: a_mitov@tu-sofia.bg

Abstract

The article is devoted to the synthesis, implementation, simulation and experimental study of a real-time *Lyapunov*-based two-degree-of-freedom model reference adaptive controller (MRAC) for an axial-piston pump. The controller of the developed real-time system determinates control signal values applied to the electro-hydraulic proportional valve. The proportional valve is an actuator for driving the swash plate swivel angle of the pump. The swash plate swivel angle determines the displacement volume of the flow rate of the pump. The MRAC is synthesized based on the experimentally identified mathematical model. To conduct the identification and experimental investigation of the controller, the authors have used an existing laboratory test setup. The comparison of the designed MRAC with conventional PI controller is performed. The control performance analysis is based on integral square error (ISE) in transient responses of the pump flow rate at different flow rate references and loads.

Keywords: *Lyapunov*; model reference adaptive control; axial-piston pump

MSC: 93C83

check for updates

Academic Editors: Yung-Hsiang Chen and Yung-Yue Chen

Received: 3 October 2025
Revised: 29 October 2025
Accepted: 31 October 2025
Published: 2 November 2025

Citation: Slavov, T.; Mitov, A.; Kralev, J. Lyapunov-Based Two-Degree-of-Freedom Model Reference Adaptive Control of Axial-Piston Pump. *Mathematics* **2025**, *13*, 3513. https://doi.org/10.3390/math13213513

Copyright: © 2025 by the authors. Licensee MDPI, Basel, Switzerland. This article is an open access article distributed under the terms and conditions of the Creative Commons Attribution (CC BY) license (https://creativecommons.org/licenses/by/4.0/).

1. Introduction

The efficiency of hydraulic drive systems largely depends on the method of the velocity regulation of the hydraulic motors (cylinders). There are two main methods of the velocity regulation, throttle and volumetric [1]. The first is based on the introduction of a variable hydraulic resistance (throttle valve, two-way or three-way flow control valve), which determines the flow rate supplied to the executive hydraulic drive motor, and the excess flow rate is separated through the main pressure-relief valve. This method of regulation has both advantages and disadvantages. The advantages are a high response performance, the ability to regulate low velocity, relatively inexpensive implementation, and easy automation. However, the general disadvantage is the large hydraulic losses, which lead to large energy losses. The second method of regulation is based on the use of a variable-displacement pump. In this way, by changing the displacement volume (at constant rotation frequency) of the pump (according to a certain control law) as much flow rate as is necessary is supplied to the executive hydraulic cylinder or motor. This leads to high energy efficiency, but there are also some disadvantages: the high cost of the pump, lower response performance (when changing the displacement volume and susceptibility to changes in the external load

acting on the driven hydraulic motor) at low velocity [2]. This makes volumetric regulation suitable for hydraulic drive systems with relatively higher power (over 4 kW).

It is not uncommon for systems with higher requirements to use a combination of the two described methods. A more modern method for dealing with the disadvantages of the two classical methods described is load sensitivity, which in turn is also associated with the use of a variable-displacement pump. The dominant factor in determining the overall efficiency of the system is the pump control performance. The most widely used in high power drives with load sensing are axial-piston pumps. The classic controllers are hydromechanical and they are allowed control according to different laws for regulating the flow rate, pressure, or power [3,4]. In mobile applications, designs of axial-piston pumps are used that allow operation in a closed circulation (hydrostatic transmission), and the controllers in them have more varieties. In industrial applications, systems with so-called secondary control [5] are more often used instead of hydrostatic transmission. Regardless of the industrial or mobile application, one of the ways to improve the control performance and energy efficiency is to replace the classic hydromechanical controller of the pump with an electro-hydraulic proportional valve [6]. On the one hand, this allows for feedback control not only by load but also by velocity. On the other hand, different types and complexities of control laws apply [7–9]. The controllers are digitally embedded in the programmable platforms [10,11]. Moreover, they can work in real time [12]. This motivates a number of researchers carrying out scientific and applied activities to seek synergy between modern control algorithms and electro-hydraulic control devices, especially for axial-piston pumps. This is evidenced by a number of developments with various advanced control algorithms such as linear-quadratic regulator (LQR), H-infinity, and μ [13–25]. Unlike conventional PID controllers [12], the advanced controller allows for higher-control performance [26]. However, the disadvantages are a more adequate mathematical model, complex synthesis, and the required larger computational resources. In this respect, the use of an adaptive controller allows a balance between a relatively easier synthesis and the need for a relatively small computational resource. Given the variation in the value and direction of the external load on the hydraulic motors, the use of adaptive control laws is appropriate [27–37].

This motivates the authors to investigate different classical and advanced control algorithms, which can be synthesized and tested both in simulation and experimental conditions.

The main goal of this article is to present the synthesis, implementation, simulation and experimental study of *Lyapunov*-based two-degree-of-freedom model reference adaptive controller of axial-piston pump.

The main contributions of this article are as follows:

- For the first time a *Lyapunov*-based two-degree-of-freedom (2DoF) model reference adaptive controller (MRAC) for real-time displacement volume regulation of an axial-piston pump is proposed.
- The stability of the designed closed loop system is theoretically proven. The tracking error convergence to zero is guaranteed in the case of bounded reference signal.
- Demonstrates experimentally closed-loop stability through the observation of tracking error convergence to zero in the presence of load-dependent variability in the pump's static gain.
- Provides a computationally efficient discretized controller implementation suitable for real-time industrial PLC operation. This controller is implemented and validated by a real-world experiment.

- The controller's performance is compared to classical PI, gradient based MRAC, and gain-scheduling adaptive controllers via experimental results on a laboratory hydraulic test bench.

This article is organized as follows: Section 2 presents the laboratory test setup description. In Section 3, the *Lyapunov-based* model reference adaptive controller design is shown, Section 4 presents the experimental evaluation of the designed controller, and Section 5 details the conclusions.

2. Laboratory Test Setup Description

For the purposes of conducting an identification experiment and the subsequent experimental study of the designed adaptive controller, the authors use an existing laboratory setup. The hydraulic diagram containing the main components of the control system is shown in Figure 1. A detailed description of the laboratory setup is given in [11] and will be presented in this article.

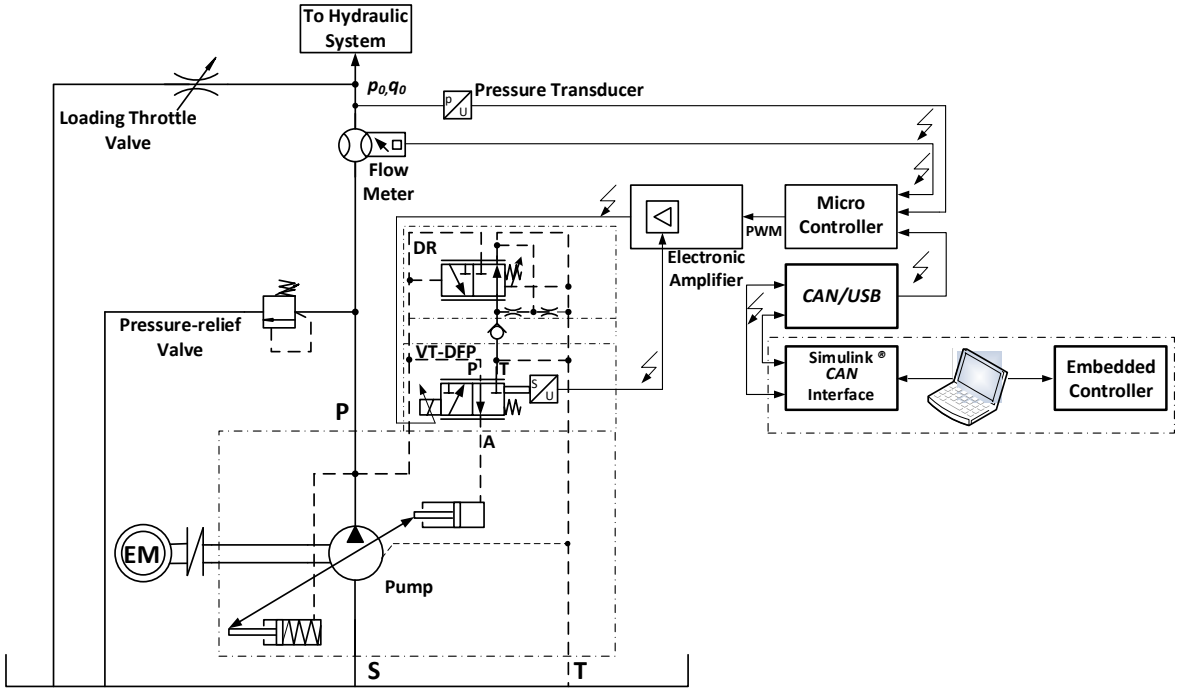


Figure 1. Hydraulic circuit diagram of the test setup.

The plant is a common model of a variable-displacement axial-piston pump A10VSO [38]. The displacement volume of the pump is 18 cm^3. The pump is driven by an electric motor with a power of 7.5 kW at a nominal speed of 1500 rpm. The pump is equipped with a proportional spool valve VT-DFP [39] serving as an electro-hydraulic actuator for changing the swash plate swivel angle, which leads to a proportional regulation of the displacement volume (resp. pump flow rate). The system is equipped with a main pressure-relief valve protecting it from pressure overload. The different load modes of the pump are set by a manually controlled adjustable precision throttle valve. The system allows for measuring flow rate and pressure in the pump discharge pipeline.

The experimental setup's control subsystem [40] has a plug-in card amplifier that is type VT-5041. It is especially intended to be used for the setup of an electro-hydraulic proportional valve. A microcontroller MC012-022 [31] sends the control signal to the amplifier. Based on the developed MATLAB/Simulink® software, various control algorithms are implemented in real time. The communication between the microcontroller and the

workstation is provided by USB/CAN interface CG150. The control actions are evaluated from the controller and sent to the power stage of the plug-in card amplifier. The plug-in card amplifier drives the proportional valve solenoid and processes the feedback signal regarding the spool position. The control algorithm is implemented as a Simulink® model. This algorithm enables displacement volume regulation in real time. The chosen sample rate of 100 Hz ensures the precise control of the pump flow rate. The realization of the laboratory experimental test setup is depicted in Figure 2.

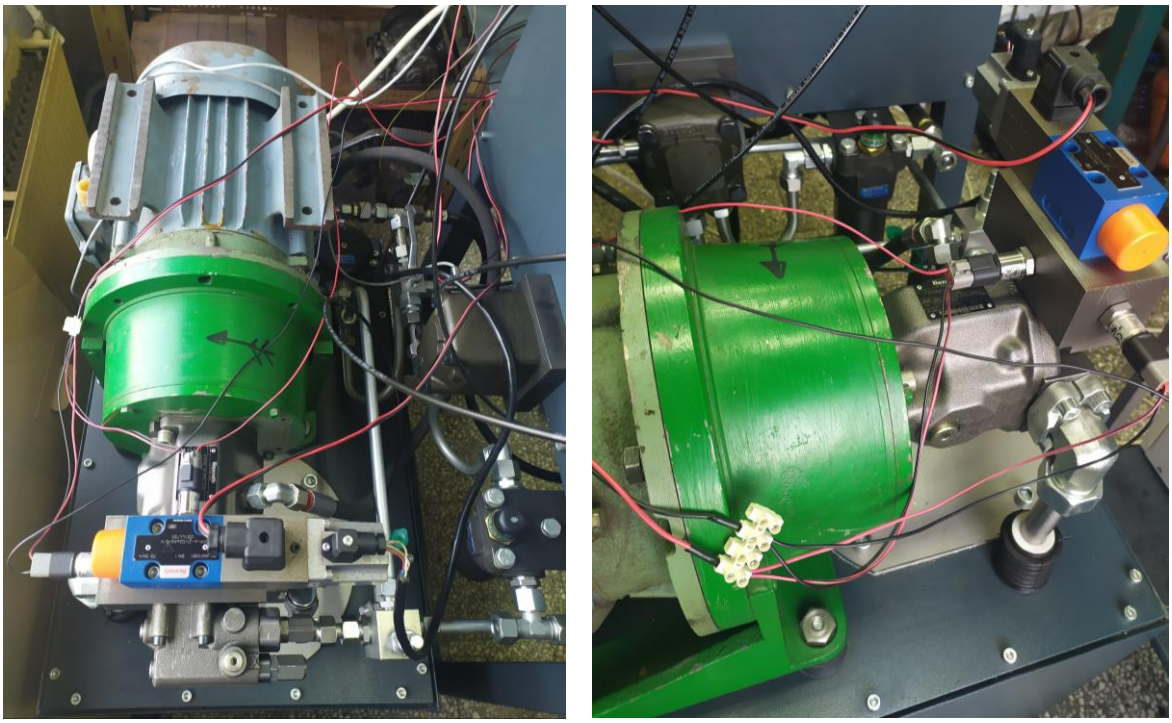


Figure 2. Real implementation of the test system.

3. Lyapunov-Based Model Reference Adaptive Controller Design

Our main purpose is to design a simple controller that can control the flow rate of axial-piston pump in a wide range of working conditions and to provide control quality and stability of a closed loop system. Moreover, this controller must be sufficiently simple in order to permit easy, real-time implementation in conventional control devices. It is well known that such a controller is the model reference adaptive controller (MRAC) designed on the basis of the Lyapunov stability criteria. The MRAC provides a control performance in case of unknown exactly plant parameters. The controller design requires sufficiently simple plant model. Thus, to estimate such a model, an experiment using a step input signal with an amplitude of 100 mV is performed. The responses are presented in Figure 3. They are measured for loadings of 1.5, 2, 2.5, 3, 4, and 5 (these loadings are realized by setting a manually controlled adjustable precision throttle valve at positions of 1.5 mm, 2 mm, 2.5 mm, 3 mm, 4 mm, and 5 mm). It is seen that the plant static gain k depends on current loading. The steady state value of flow rate for loading 5 is approximately 21.5 L/min, since one for loading 1.5 is approximately 12 L/min. Thus, the static gain of the pump k takes values in range $k \in [0.12, 0.215]$ (the amplitude of input signal is 100 mV). As can be seen in Figure 3, the settling time of the axial-piston pump in respect to the flow rate varies between 0.06 s and 0.09 s for a complete working range. Also, it

is obvious that the axial-piston dynamics can be approximated sufficiently well by a first order differential equation

$$\dot{y}(t) = -\frac{1}{T}y(t) + \frac{k}{T}u(t), \tag{1}$$

where $y(t)$ is the measured axial-piston pump flow rate and $u(t)$ is the control action.

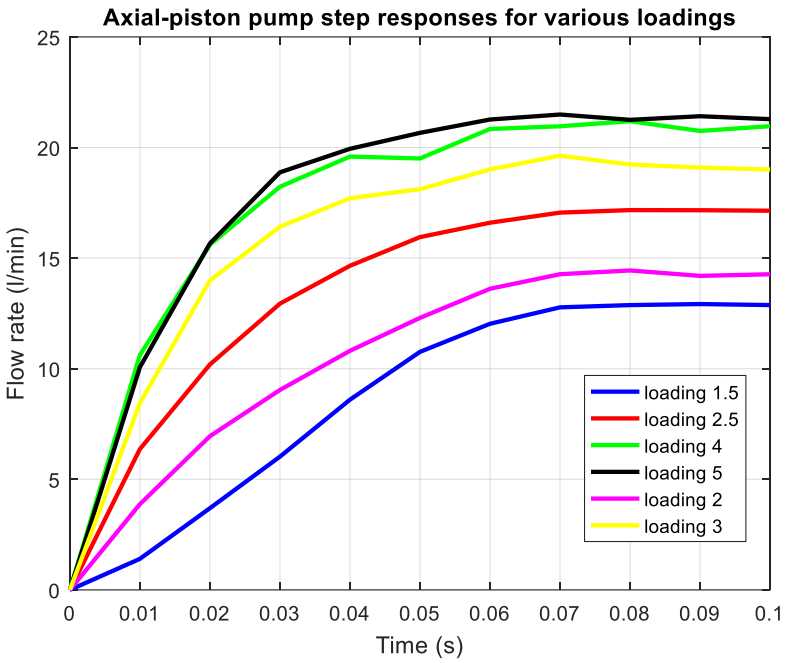


Figure 3. Flow rate step responses for different loadings.

Due to the approximately constant value of settling time for all loadings, the rough approximation of plant dynamics can be achieved with time constant $T = 0.018$ s, but it should be noted that its exact value is unknown. For example, the static gain for loading 2.5 is $k = 0.17$. The measured step response of model (1) for loading 2.5 is presented in Figure 4.

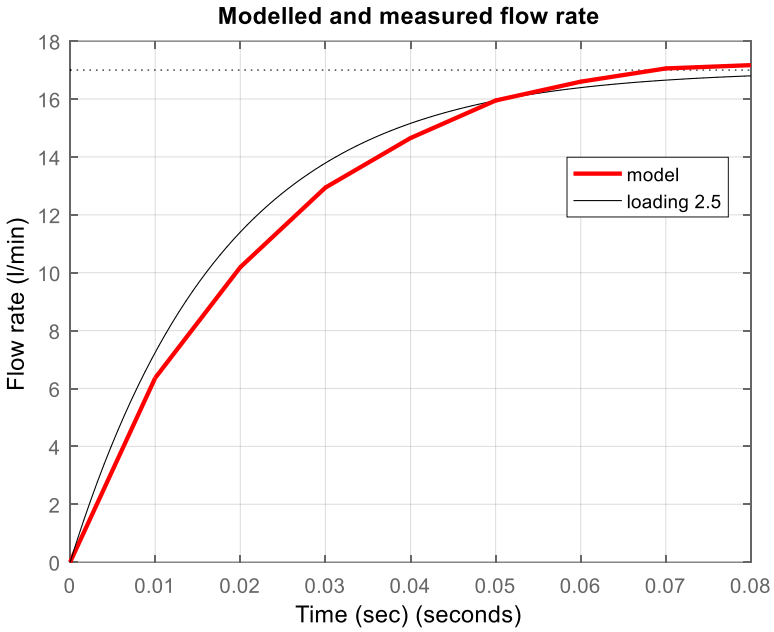


Figure 4. Axial-piston pump flow rate evaluated by model (1) and measured axial-piston pump flow rate at loading 2.5.

As can be seen from Figure 4, the model (1) approximates plant dynamics for loading of 2.5. In order to compensate for unknown values of plant static gain and plant time constant for various loading conditions the two-degree-of-freedom MRAC is designed. Its feedback and feedforward dynamics are given by

$$u(t) = hr(t) - fy(t), \tag{2}$$

where $r(t)$ is desired flow rate (reference signal), h and f are controller parameters. The closed loop system dynamics is described by

$$\dot{y}(t) = -\frac{(1+kf)}{T}y(t) + \frac{kh}{T}r(t). \tag{3}$$

The MRAC design goal is to determine the controller parameters in such a manner that output signal $y(t)$ converges to output signal of reference model

$$\dot{y}_M(t) = -\frac{1}{T_M}y_M(t) + \frac{1}{T_M}r(t), \tag{4}$$

where $y_M(t)$ is the reference model output and $T_M = 0.005$ s is the reference model time constant. The reference model static gain is chosen to take the value of 1, because the pump flow rate should be equal to the desired flow rate in steady state mode. The value of T_M is smaller than one of T in order to obtain smaller settling time of closed loop system. From Equations (3) and (4) it is seen that if

$$f = \frac{T - T_M}{T_M k}, h = \frac{T}{T_M k}, \tag{5}$$

then the closed loop dynamics will be the same as one for reference model (4). The problem is that the exact values of plant model parameters T and k are unknown. Thus, instead of "ideal" controller parameters f and h in control signal (2), their time varying estimates $\hat{f}(t)$ and $\hat{h}(t)$ are used. The difference between the dynamics of the reference model and closed loop system is described by equation

$$\dot{e}(t) = \dot{y}(t) - \dot{y}_M(t), \tag{6}$$

where $e(t) = y(t) - y_M(t)$ is the model reference error. After substituting the measured output and reference model output from Equations (3) and (4) into Equation (6), one obtains

$$\dot{e}(t) = -\frac{1+k\hat{f}(t)}{T}y(t) + \frac{k\hat{h}(t)}{T}r(t) + \frac{1}{T_M}y_M(t) - \frac{1}{T_M}r(t). \tag{7}$$

After elementary conversions one obtain

$$\dot{e}(t) = -\frac{1+k\hat{f}(t)}{T}y(t) + \frac{k\hat{h}(t)}{T}r(t) + \frac{1}{T_M}y_M(t) - \frac{1}{T_M}r(t) + \frac{1}{T_M}y(t) - \frac{1}{T_M}y(t), \tag{8}$$

$$\dot{e}(t) = -\frac{1}{T_M}e(t) + (\frac{1}{T_M} - \frac{1+k\hat{f}(t)}{T})y(t) + (\frac{k\hat{h}(t)}{T} - \frac{1}{T_M})r(t). \tag{9}$$

Taking into account expression (5), Equation (9) can be rewritten as follows

$$\dot{e}(t) = -\frac{1}{T_M}e(t) + \frac{k}{T}(\widetilde{h}(t)r(t) - \widetilde{f}(t)y(t)), \tag{10}$$

where $\widetilde{h}(t) = \hat{h}(t) - h, \widetilde{f}(t) = \hat{f}(t) - f$ are errors of controller parameters.

Lemma 1. *Let $k > 0, T > 0$ are unknown plant gain and time constant and; $T_M > 0$ is known reference model time constant and $\gamma_f > 0, \gamma_h > 0$ are constants and*

$$\begin{array}{l} \dot{\hat{h}}(t) = -\widetilde{\gamma}_h e(t) r(t),\ \widetilde{\gamma}_h = \frac{T}{k\gamma_h} > 0, \\ \dot{\hat{f}}(t) = \widetilde{\gamma}_f e(t) y(t),\ \widetilde{\gamma}_f = \frac{T}{k\gamma_f} > 0 \end{array}. \tag{11}$$

Then the model reference error $e(t)$ is bounded. Moreover, if the reference signal $r(t)$ is bounded then

$$\lim_{t\to\infty} e(t) \to 0. \tag{12}$$

Proof. The possible candidate for *Lyapunov* function for system (9) is

$$V(e(t), \hat{f}(t), \hat{h}(t), t) = \frac{1}{2}e^2(t) + \frac{\gamma_f}{2}\left(\frac{1}{T_M} - \frac{1 + k\hat{f}(t)}{T}\right)^2 + \frac{\gamma_h}{2}\left(\frac{k\hat{h}(t)}{T} - \frac{1}{T_M}\right)^2, \tag{13}$$

where $\gamma_f > 0, \gamma_h > 0$ are constants.

It is clearly that V is positive definite, i.e.,

$$\begin{array}{l} V = 0\ for\ e = 0, \hat{f} = f, \hat{h} = h \\ V > 0\ for\ e \neq 0, \hat{f} \neq f, \hat{h} \neq h \end{array}. \tag{14}$$

It is known that the $V(e(t), f(t), h(t), t)$ is a Lyapunov function if its total derivative respect to time satisfies condition

$$\dot{V}(e(t), \hat{f}(t), \hat{h}(t), t) < 0. \tag{15}$$

The time derivative of (13) is

$$\dot{V}(e(t), \hat{f}(t), \hat{h}(t), t) = e(t)\dot{e}(t) - \gamma_f \frac{k}{T}\left(\frac{1}{T_M} - \frac{1 + k\hat{f}(t)}{T}\right)\dot{\hat{f}}(t) + \gamma_h \frac{k}{T}\left(\frac{k\hat{h}(t)}{T} - \frac{1}{T_M}\right)\dot{\hat{h}}(t). \tag{16}$$

After substituting (9) in (16) one obtains

$$\begin{array}{l} \dot{V}(e(t), \hat{f}(t), \hat{h}(t), t) = -\frac{1}{T_M}e^2(t) + \left(\frac{1}{T_M} - \frac{1+k\hat{f}(t)}{T}\right)e(t)y(t) + \left(\frac{k\hat{h}(t)}{T} - \frac{1}{T_M}\right)e(t)r(t) \\ -\gamma_f \frac{k}{T}\left(\frac{1}{T_M} - \frac{1+k\hat{f}(t)}{T}\right)\dot{\hat{f}}(t) + \gamma_h \frac{k}{T}\left(\frac{k\hat{h}(t)}{T} - \frac{1}{T_M}\right)\dot{\hat{h}}(t) \end{array}. \tag{17}$$

By regrouping (17) one obtains

$$\begin{array}{l} \dot{V}(e(t), \hat{f}(t), \hat{h}(t), t) = -\frac{1}{T_M}e^2(t) + \left(\frac{1}{T_M} - \frac{1+k\hat{f}(t)}{T}\right)\left(e(t)y(t) - \gamma_f \frac{k}{T}\dot{\hat{f}}(t)\right) \\ +\left(\frac{k\hat{h}(t)}{T} - \frac{1}{T_M}\right)\left(e(t)r(t) + \gamma_h \frac{k}{T}\dot{\hat{h}}(t).\right) \end{array} \tag{18}$$

After substitution of (11) into (18) the time derivative of (13) is

$$\dot{V}(e(t), \hat{f}(t), \hat{h}(t), t) = -\frac{1}{T_M}e^2(t) \leq 0. \tag{19}$$

Clearly $e, \hat{f}$ and $\hat{h}$ are bounded ($V(t) \leq V(0)$). If the reference signal $r(t)$ is bounded, then the $y_M(t)$ from Equation (4) is bounded. Therefore output $y(t)$ is bounded too (due to

$y(t) = e(t) + y_M(t)$). Thus, as can be seen from Equation (9) the $\dot{e}(t)$ is also bounded. The second time derivative of the *Lyapunov* function (13) is

$$\ddot{V}(e(t), \hat{f}(t), \hat{h}(t), t) = -2\frac{1}{T_M} e\dot{e}, \tag{20}$$

that is bounded too and $\dot{V}$ is uniformly continuous. Therefore, according to *Barbalat's* lemma, the condition (12) holds. □

Corollary 1. *Taking into account expressions (11) and (12) it is concluded that*

$$\lim_{t\to\infty} \dot{\hat{h}}(t) \to 0, \lim_{t\to\infty} \dot{\hat{f}}(t) \to 0, \Rightarrow \lim_{t\to\infty} \hat{h}(t) \to const, \lim_{t\to\infty} \hat{f}(t) \to const. \tag{21}$$

Expression (21) does not guarantee that the controller parameters converge to ''ideal" values (5). Indeed, the tracking error $e(t)$ converge to zero and it is the output of a stable system (1), so the input signal of this system $\frac{k}{T}(\widetilde{h}(t)r(t) - \widetilde{f}(t)y(t))$ should converge to zero. Also $\widetilde{h}(t)$ and $\widetilde{f}(t)$ converge to constant values $\overline{h}$ and $\overline{f}$ that should satisfy

$$\overline{h}r(t) - \overline{f}y(t) = 0. \tag{22}$$

It should be noted that if the reference signal is constant $r(t) = \overline{r} \neq 0$ for $t \in (0, \infty)$ then $y = y_M = \overline{r}$ for $t \to \infty$ and the following is hold

$$\overline{r}(\overline{h} - \overline{f}) = 0. \tag{23}$$

Equation (23) only implies $\overline{h} = \overline{f}$ which gives an infinite number of solutions over a straight line and does not guarantee that $\overline{h} = 0$ and $\overline{f} = 0$. The expression (22) can be written as

$$\begin{aligned} &\nu^T \eta = 0, \\ &\nu^T = \begin{bmatrix} r(t) & -y(t) \end{bmatrix}, \eta = \begin{bmatrix} \overline{h} & \overline{f} \end{bmatrix}^T. \end{aligned} \tag{24}$$

It is well known [41] that if for any t, there are $L, \alpha > 0$ such that

$$\int_t^{t+L} \nu\nu^T d\tau \geq \alpha I, \tag{25}$$

then ν is persistently exciting that guarantee $\eta = 0$. It can be shown that the designed control system condition (25) is satisfied if the reference signal contains at least one sinusoid. It should be noted that in a hydraulic control system, the most commonly used reference signals are constant or piecewise constant that led to violation of (25) and $\overline{h} = const \neq 0$, and $\overline{f} = const \neq 0$. Nevertheless, the control system has excellent tracking performance (the control system output signal tracks the reference model output). In more rare cases in hydraulic control, the reference signal is periodic rectangular pulses, then the controller parameters converge to their "ideal" values.

Constants $\widetilde{\gamma}_h$ and $\widetilde{\gamma}_f$ in expressions (11) are algorithm tunable parameters. Larger values of $\widetilde{\gamma}_h$ and $\widetilde{\gamma}_f$ lead to fast adaptation process but to large oscillations in the adaptation transient response. Moreover, in real-world implementation, the values $\widetilde{\gamma}_h$ and $\widetilde{\gamma}_f$ are limited by measurement noise and actuator amplitude limitations. However, for real-

time implementation of the model reference adaptive control algorithm, derivatives in Equation (13) are approximated by first backward difference

$$\begin{array}{l} h(k) = h(k-1) - \widetilde{\gamma}_{hd} e(k) r(k),\ \widetilde{\gamma}_{hd} = \widetilde{\gamma}_h T_s, h(0) = h_0 \\ f(k) = f(k-1) + \widetilde{\gamma}_{fd} e(k) y(k),\ \widetilde{\gamma}_{fd} = \widetilde{\gamma}_f T_s, f(0) = f_0, \end{array} \tag{26}$$

with $T_s = 0.01$ s is sample time. It should be noted that Equation (26) represented discrete time realization of continuous control law. After discretization of (4) and taking into account dynamics of zero order holder the discrete time reference model is described by

$$y_M(k) = \frac{0.8647}{q - 0.1353} r(k), \tag{27}$$

where q is time shift operator. Applying operator q to Equation (26) one obtains

$$\begin{array}{l} h(k) = -\widetilde{\gamma}_{hd} \frac{1}{q-1} e(k) r(k), \\ f(k) = \widetilde{\gamma}_{fd} \frac{1}{q-1} e(k) y(k) \end{array} . \tag{28}$$

Finally, the block diagram of the adaptive closed loop system is presented in Figure 5.

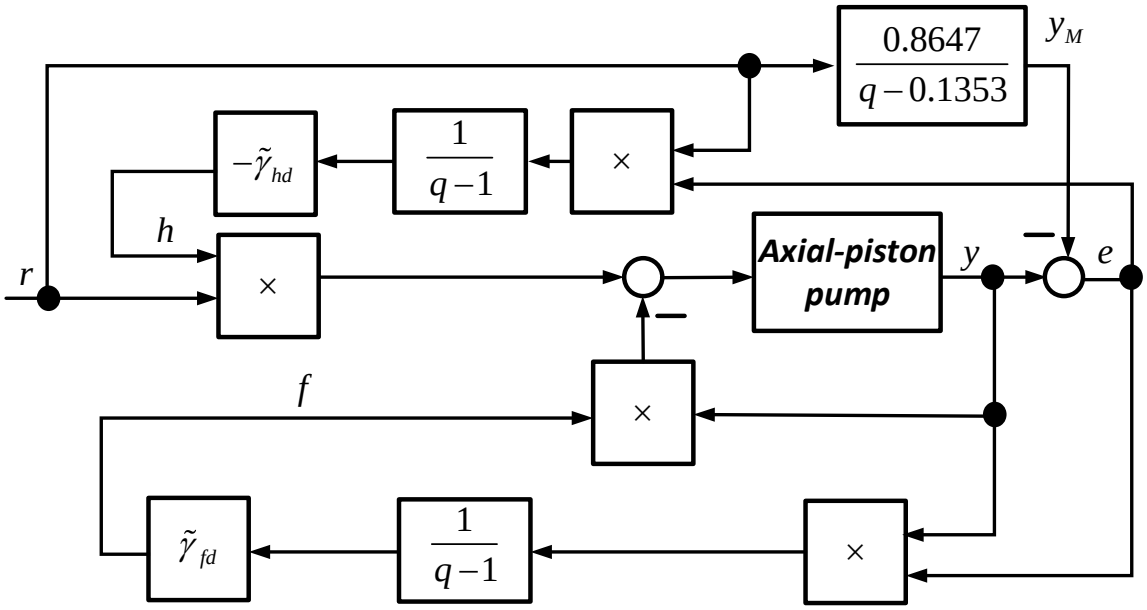


Figure 5. Block scheme of *Lyapunov*-based model reference adaptive control system.

The values $\widetilde{\gamma}_{hd} = 0.3, \widetilde{\gamma}_{fd} = 0.2$ are experimentally determined. They provide a good compromise between oscillations in control signal and adaptation time.

In order to investigate the quality of the designed controller and to investigate the possibilities of an adaptive control approach for real-time control of the axial-piston pump, a comparison with the previously designed model reference adaptive controller (MRAC) [42] and gain scheduling adaptive controller (GSAC) [43] is performed.

The previously designed MRAC uses the reference model (27) and forms the control signal according to Equation (29). The controller parameters $\hat{h}_m(k)$ and $\hat{f}_m(k)$ are evaluated by the expressions [42]

$$\begin{array}{l} \hat{h}_m(k+1) = \hat{h}_m(k) - T_0 \gamma_{hm} e(k) \frac{0.8647}{(q-0.1353)} r(k),\ \gamma_{hm} = 0.8 \\ \hat{f}_m(k+1) = \hat{f}_m(k) + T_0 \gamma_{fm} e(k) \frac{0.8647}{(q-0.1353)} y(k),\ \gamma_{fm} = 1.5. \end{array} \tag{29}$$

The GSAC uses the linear parameter-varying model of the axial-piston pump [43]

$$W(s) = \frac{k(r)}{0.018s + 1}, \tag{30}$$

where

$$k(r) \approx \frac{r}{100}. \tag{31}$$

The control signal is evaluated by equations

$$\begin{array}{l} u(k) = K_p(r)e_{fl}(k) + u_i(k) \\ u_i(k+1) = u_i(k) + K_i(r)T_0e_{fl}(k) - K_{aw}T_0(u(k) - u_{sat}) \end{array}, \tag{32}$$

where $e_{fl}(k) = r(k) - y(k)$ is the reference error, k_{aw} is an anti-wind-up gain that is chosen experimentally to achieve proper wind-up compensation and u_{sat} is either the control signal upper bound or control signal lower bound:

$$u_{sat} = \begin{cases} 1000, u \geq 1000 \\ u, 0 < u < 1000 \\ 0, u \leq 0 \end{cases}. \tag{33}$$

The controller parameters are evaluated as follows:

$$K_p(r) = \frac{134}{r}, K_i(r) = \frac{21600}{r}. \tag{34}$$

4. Experimental Evaluation of *Lyapunov-Based* MRAC

4.1. Testbench Controller Implementation

The testbench architecture for controller implementation represents a distributed real-time control system where the designed controller, built and tested in Simulink, operates in direct coordination with a Danfoss industrial PLC [44] via a Controller Area Network (CAN) bus. In this configuration, the Simulink environment functions not merely as a simulation platform, but as a real-time controller executing compiled code that interacts continuously with the physical PLC hardware. The CAN bus provides a deterministic communication backbone that allows the timely exchange of control commands, sensor feedback, and synchronization signals between the two systems.

To ensure that both the PLC and the Simulink-based controller remain in synchronization during execution, the PLC periodically transmits a synchronization packet in blocking communication mode over the CAN. This signal effectively blocks the execution of the Simulink model until the synchronization packet arrives. Then, the model logic is executed as fast as the host CPU allows to generate a response packet to the PLC in the same sampling time. In this way, the system imposes a hardware-driven timing constraint that guarantees deterministic sampling and response intervals. In practice, this means the Simulink algorithm only proceeds to its next computation step when the synchronization signal from the PLC arrives, achieving precise cooperative timing similar to a real-time scheduling system. Of course, such architecture has limited application to laboratory setups for rapid prototyping due to the general purpose operating system at the host.

The Simulink model hosts the adaptive controller and runs with a fixed sampling rate of 100 Hz, which provides a sufficiently high resolution for precise pump flow regulation. This sampling frequency matches flow rate sensor capabilities and ensures that even fast variations in hydraulic flow can be corrected by the control algorithm. In operation, the control outputs computed by the Simulink algorithm are transmitted to the VT-5041 amplifier's power stage, which in turn actuates the proportional valve solenoid.

4.2. Experimental Results

The performance of adaptive controllers is examined for a wide range of loading conditions and compared with a previously designed MRAC, GSAC, and conventional PI controller. Flow rate regulation in four control systems using a *Lyapunov*-based model reference adaptive control system (LMRAC), model reference adaptive control system (MRAC), gain scheduling adaptive control system (GSAC), and control system with conventional PI controller (PI) was tested for highest loading imposed on the pump output, which is presented in Figure 6. The desired flow rate in this mode is between 14 and 17 L/min.

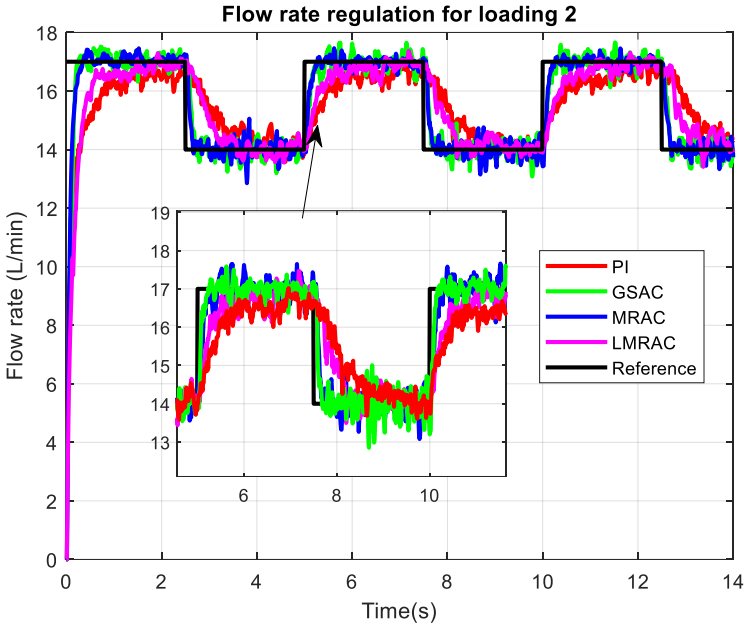


Figure 6. Axial-piston pump flow rate control at loading 2.

The controllers show marked differences in their dynamic and steady-state behaviors. The initial rise times for all controllers are rapid. The LMRAC and PI controllers closely mirror each other, showing no overshoot, moderate settling times above 0.5 s, and relatively low noise sensitivity. The GSAC and MRAC exhibit slightly faster rise times compared to LMRAC, with GSAC tending to be more aggressive, resulting in minor overshoots.

Similarly, Figures 7–9 demonstrate controller behavior for lower loading conditions corresponding to different levels of shunt valve opening in millimeters. For loading 3, where pump output is less restricted and the throttle valve is more open than loading 2, the difference between adaptive controllers (LMRAC, MRAC, GSAC) becomes less pronounced in terms of settling time. Since the resistance of the pump output is reduced, the adaptive controllers achieve reference value in less than 0.25 s, which is exceptionally fast for pump output regulation. The GSAC experienced more oscillations at a higher flow rate reference with an amplitude up to 0.5 L/min, while the MRAC and LMRAC have similar lower steady state errors. However, it should be noted that an initial overshoot for the MRAC during the starting of the system is observed. while such overshoot is absent for the LMRAC. As a conventional PI controller is not tuned for this particular loading, it experienced a considerable increase in settling time, though with a more damped response with respect to noise, which is expected due to the shift in the open loop frequency response to lower frequencies.

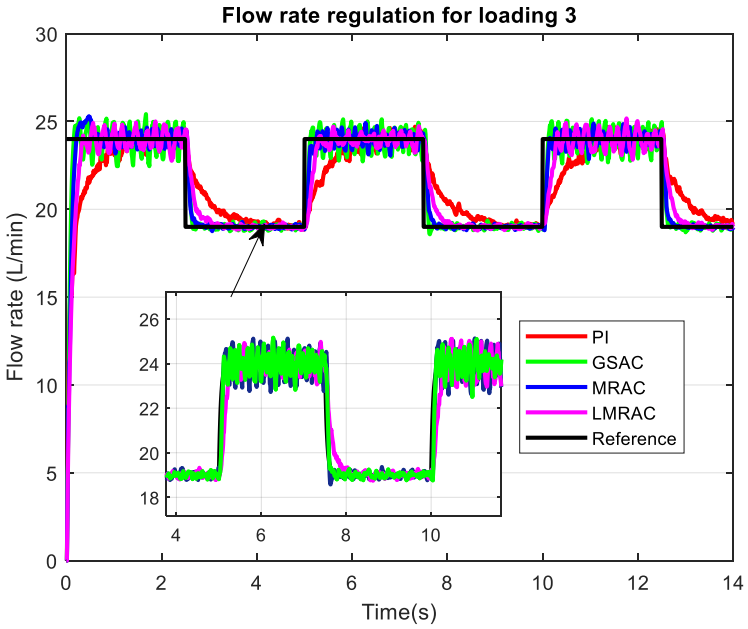


Figure 7. Axial-piston pump flow rate control at loading 3.

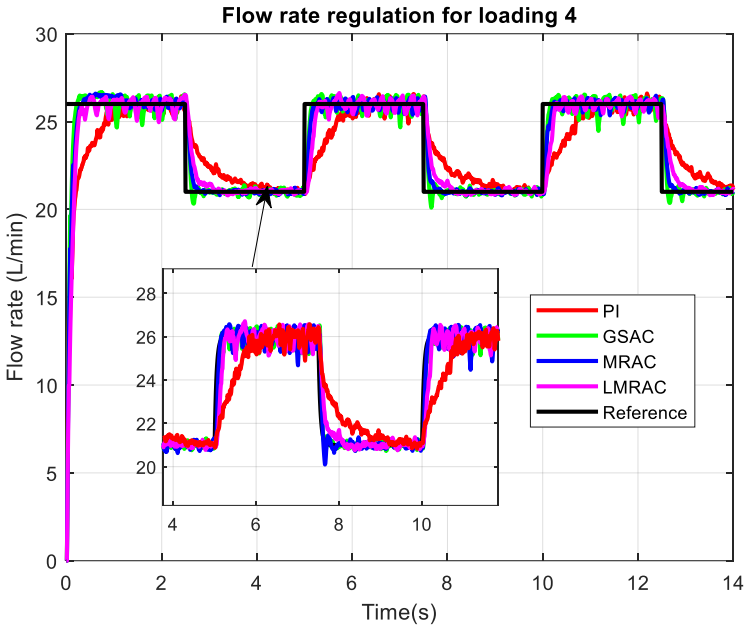


Figure 8. Axial-piston pump flow rate control at loading 4.

For loading 4 (corresponding to less restriction to output flow compared to loading 3) we observed more damping behavior of the adaptive controllers with respect to the steady state oscillations. Here, LMRAC demonstrated a little bit higher steady state deviations than MRAC during the startup step, which became reduced in the following reference changes. However, the MRAC, again, had an obvious overshoot up to 0.3 L/min during the startup step, which became corrected with time as well. The conventional PI controller continued to underperform compared to adaptive controllers, due to its more conservative tuning required to handle variable load conditions.

Lowest loading 5 corresponds to minimal restriction to pump output with the same range for flow rate commands as we had for loading 4. The behavior of the adaptive controllers was again similar with a very fast rise time and settling time. The steady state noise oscillations at high flow rates were similar between all controllers, with the GSAC

showing increased oscillation amplitude during the third reference step. That points to its limited robustness. The MRAC continued to experience a startup overshot of about 0.3–0.5 L/min which was corrected with following operation of the controller. The PI controller demonstrated a faster response compared to higher loading conditions but was still far behind the adaptive counterparts.

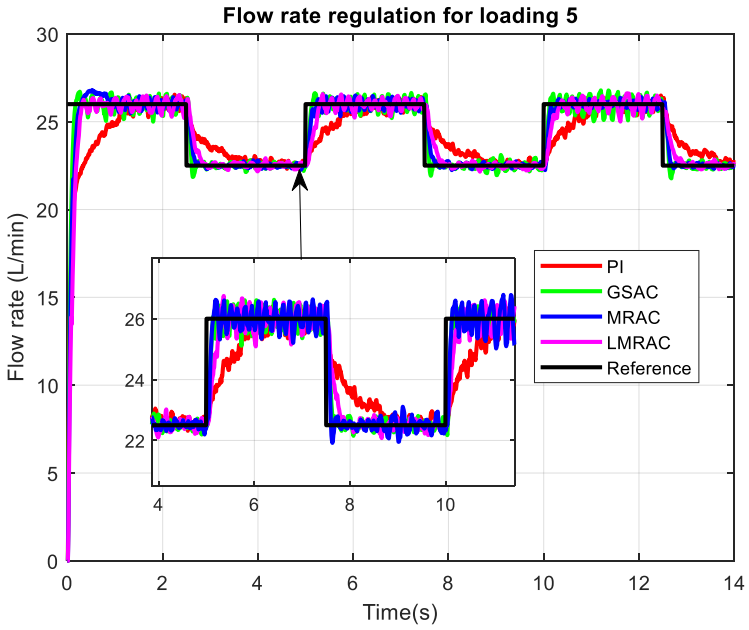


Figure 9. Axial-piston pump flow rate control at loading 5.

The calculated control signals for a *Lyapunov*-based model reference adaptive control system under different loading conditions are visualized in Figure 10 and control signals for the PI controller for the same loading conditions are in Figure 11. As the load increased for LMRAC, the control signal amplitude first rises accordingly, indicating the controller's adaptive compensation for the varying plant gain. However, when reaching the highest loading, the control amplitude became reduced again, notably to compensate for the reduced stability margin of the pump output and susceptibility to oscillatory behavior. Across all loadings from 3 to 5, the controller exhibited rapid transitions in response to the step changes in reference.

Notable differences emerge in the control action for the PI controller compared to the adaptive controllers. The PI controller exhibited consistent low frequency behavior with reduced, but not absent, noise sensitivity. The signal shape demonstrates the inherent limitations of fixed-gain regulation. By keeping the same waveform structure, yet not able to fully compensate for changing plant gain, the result is a bigger output error and less differentiated response among loading curves.

The extension of loading on the system can be appreciated by looking at pump output pressures presented in Figure 12 for LMRAC and in Figure 13 for the conventional PI controller. The pressure increases exponentially with loading from 20 bars to above 100 bars, intermittently reaching 120 bars, which is limited by the pressure-relief valve acting in this range. The output pressure decreases progressively from loading 2 to loading 5, since less restriction yields lower pressure for the same flow setpoint. The controller tracks the reference-induced step changes with transitions between high- and low-pressure states, maintaining the pressure level appropriate to each loading curve. Pressure overshoot and steady-state oscillations are more visible at the highest pressure, reflecting the challenge of controlling more restricted flow and greater pump effort.

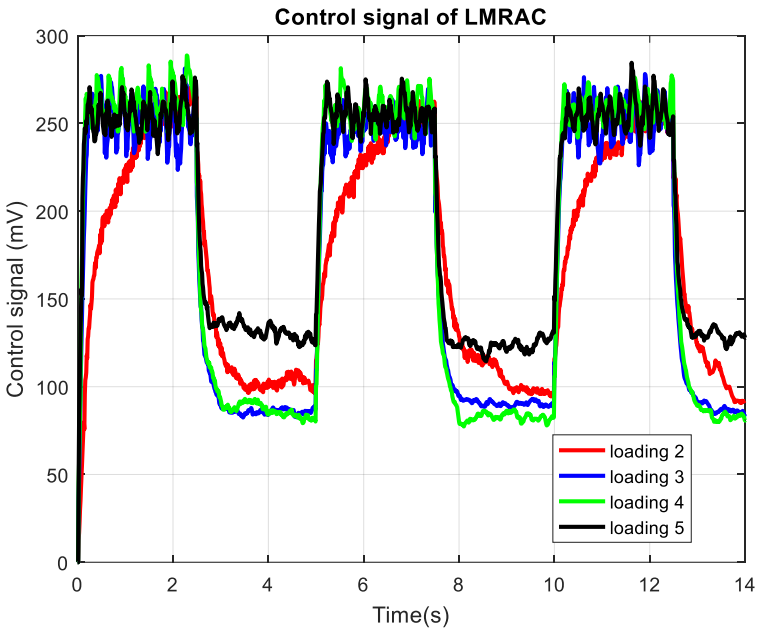


Figure 10. Control signal of LMRAC for various loadings.

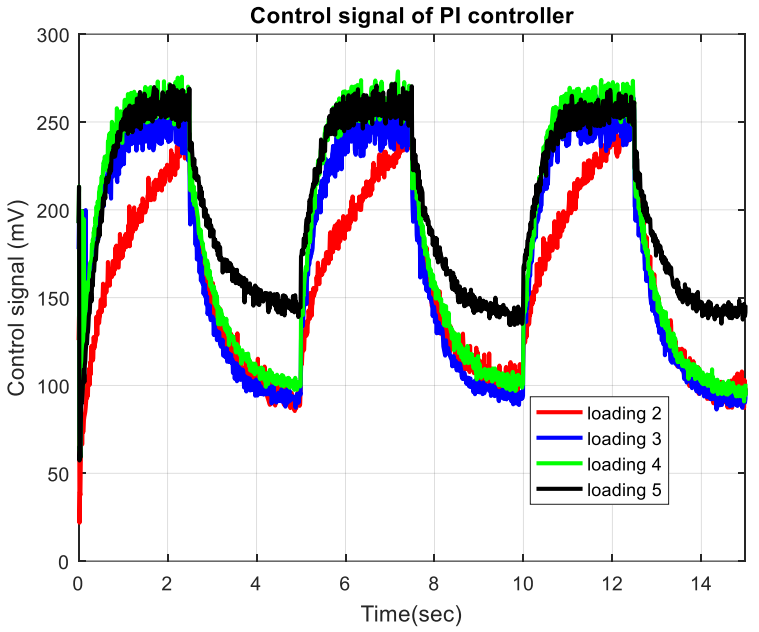


Figure 11. Control signal of PI controller for various loadings.

In order to numerically compare the control system performance, the following index is introduced

$$err(k) = \frac{1}{(t_f - t_0)} \sum_{k=t_0}^{t_f} \Big(y_{fl}(k) - r(k) \Big)^2 + \lambda u^2(k), \quad \lambda = 1 \times 10^{-7}. \tag{35}$$

It should be noted that the axial-piston pump flow rate takes values between 10 L/min and 26 L/min, whereas the control signal takes values in range 0–1000 mV. So, the first term in (35) will take values in range $10^2 \div 10^3$, while the second term will take values up to 10^9. By weighting coefficient λ the values of the second term are scaled to the values of the first term and the control signal has approximately the same weight as one of pump flow. Table 1 presents values of index (35) for the four control systems under various loading conditions. The index (35) is evaluated for $t_0 = 2.5$ s and $t_f = 14$ s according to the

results in Figures 6–9. The results clearly demonstrate that the *Lyapunov* MRAC consistently achieves lower index (35) values across all tested loadings (2, 3, 4, and 5), indicating superior tracking accuracy and transient performance compared to the PI controller. Specifically, the index (35) for LMRAC ranges from 4.0497 to 4.5942, while the PI controller's index (35) is significantly higher, ranging from 4.3930 to 6.0027, with the largest performance gap observed at loading 4. This highlights the advantage of the *Lyapunov*-based MRAC in adapting to varying system dynamics and maintaining robust control quality, especially as the system load changes, whereas the PI controller's fixed parameters result in degraded performance under such variations. It is seen that the three adaptive control systems have similar performance. For loading 2, the smallest value of index (35) value is for LMRAC, since for loading 5 the lowest value is for GSAC, but for the whole working range the values are very close. The advantage of LMRAC is that the stability of the system is theoretically guaranteed. From a numerical point of view, all three adaptive systems are sufficiently simple for real-time implementation with a conventional microcontroller.

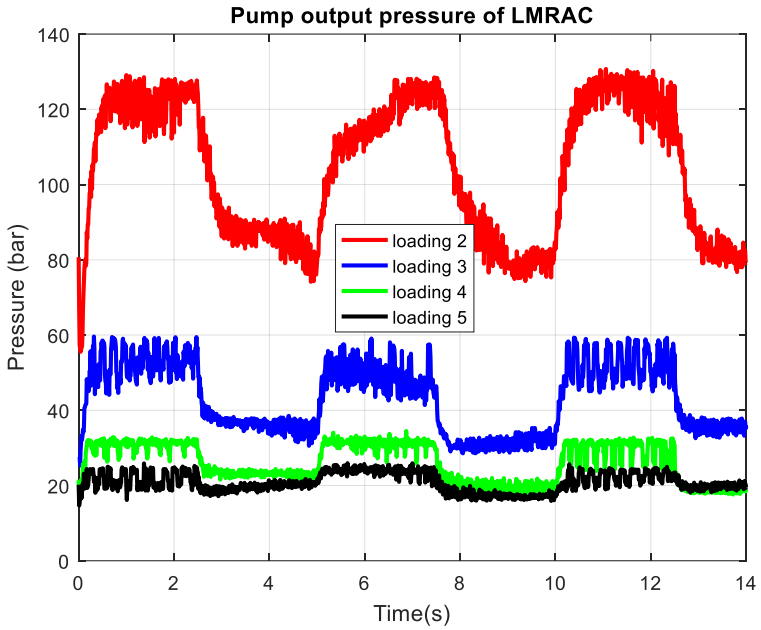


Figure 12. Axial-piston pump output pressure for *Lyapunov*-based MRAC system at various loadings.

Table 1. Performance index of control systems with various controllers.

Controller Type	Index (35)			
	Loading 2	**Loading 3**	**Loading 4**	**Loading 5**
LMRAC	4.3479	4.2370	4.0497	4.5942
PI	4.3930	5.6052	6.0027	5.7993
MRAC	4.3844	4.1937	3.8419	4.2449
GSAC	4.0769	4.3559	4.1074	4.2826

In order to investigate the developed *Lyapunov-based* adaptive controller in different working modes, experiments with dynamically changing load conditions were performed. The realization of the dynamic load pressure disturbance is performed by manual adjustment of precise throttle valve. This is performed in both directions (open/close) for random time moments with various adjustment velocities. Figure 14 shows the measured flow rate of the axial-piston pump for LMRAC and PI control systems in case of significant variations in hydraulic loading, with multiple reference signal changes appearing throughout the

experiment. Despite these dynamic disturbances, the flow rate remains tightly regulated and follows the reference trajectory with a settling time that is smaller than 250 ms without undershoot and overshoot. The PI controller reacts slower than the adaptive controller.

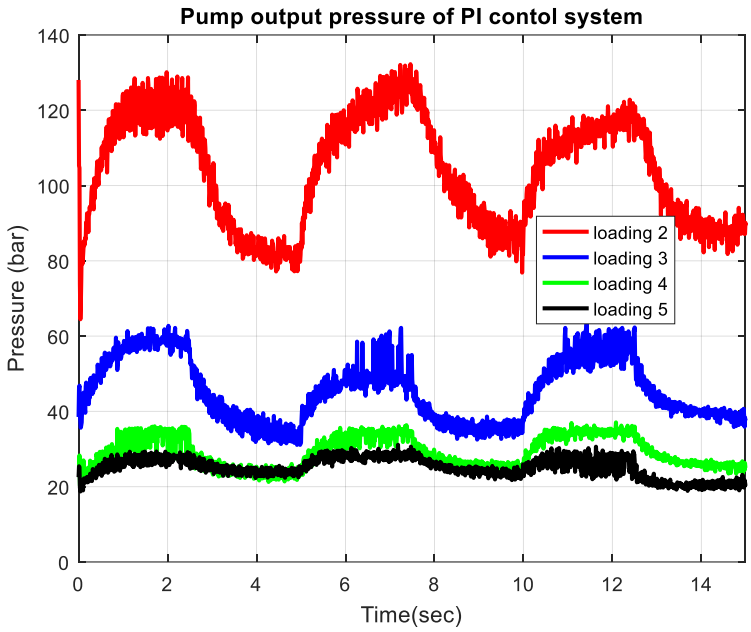


Figure 13. Axial-piston pump output pressure for PI controller system at various loadings.

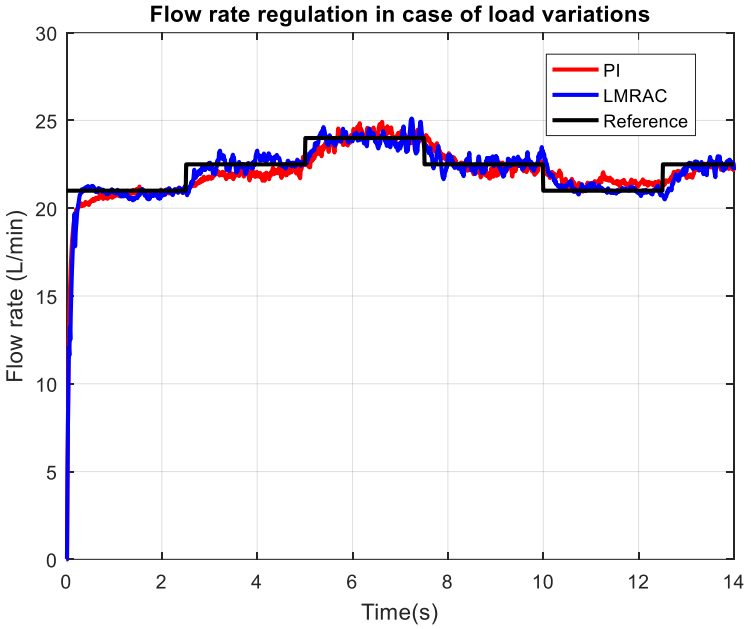


Figure 14. Axial-piston pump flow rate at various loadings.

The axial-piston pump output pressure in case of dynamically changing load is presented in Figure 15. This result reveals real-time insight into how the control system changes with various types of load fluctuations. During the experiment, the pump output pressure exhibits marked transient peaks and grooves that correspond to each load disturbance. Figure 16 depicts the control action of the LMRAC in response to dynamically varying load conditions. As can be seen, the control signal changes rapidly in order to compensate for each pump load. In this way, the system maintains the desired flow rate level. The control signal for the adaptive controller is smoother than one for the conventional PI controller,

which is more appropriate for the operational mode of the electro-hydraulic proportional spool valve.

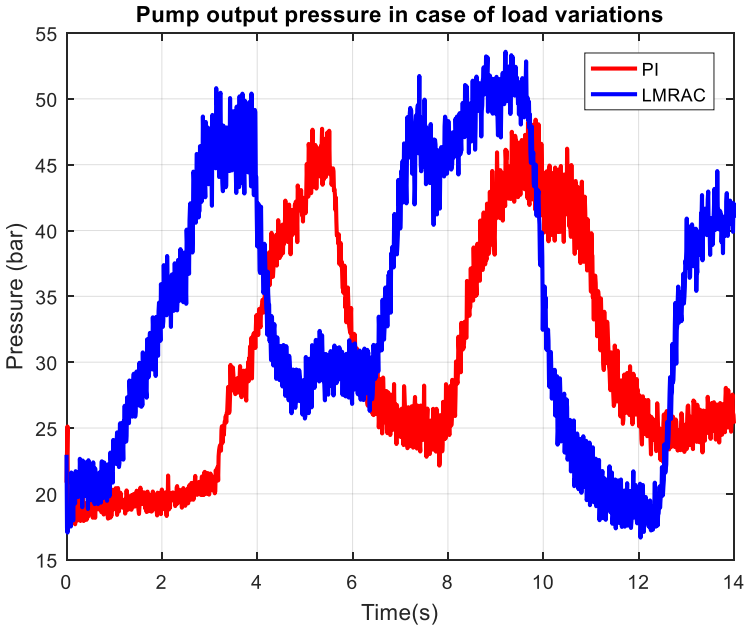


Figure 15. Axial-piston pump output pressure at various loadings.

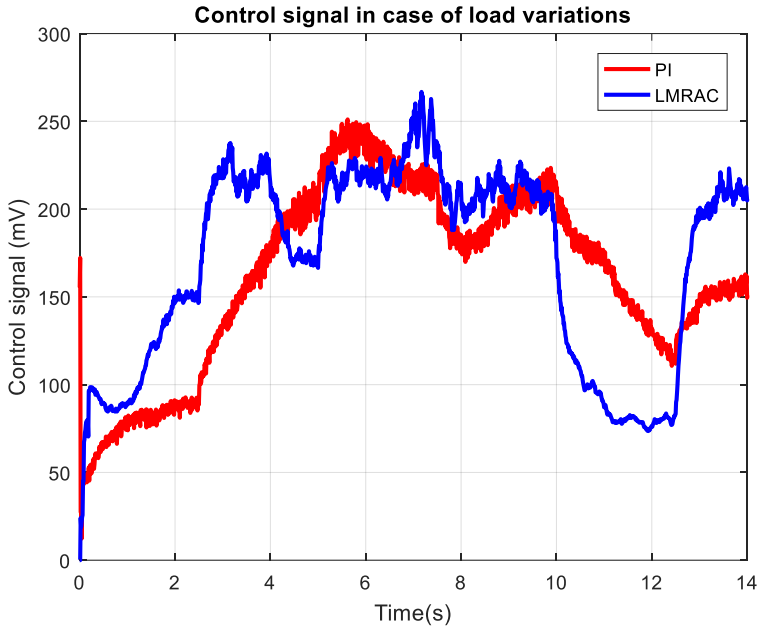


Figure 16. Axial-piston pump control at various loadings.

5. Conclusions

The developed *Lyapunov*-based two-degree-of-freedom model reference adaptive controller (LMRAC) demonstrates significant theoretical and practical advancements in axial-piston pump control. By employing *Lyapunov*'s direct stability method, the controller architecture integrates a first-order reference model and adaptively adjusts feedforward and feedback gains through discrete-time update laws derived from stability criteria. The adaptation mechanism ensures asymptotic tracking while compensating for load-dependent variations in the pump's static gain. This theoretical framework guarantees closed-loop stability by constructing a *Lyapunov* function whose time derivative remains negative

definite, forcing the tracking error to converge to zero. The discretized implementation maintains computational efficiency for real-time operation on industrial PLCs, balancing rapid parameter convergence with noise resilience through carefully tuned adaptation rates.

Experimental validation across loading conditions confirmed the controller's superiority over conventional PI control, with integral square error (ISE) reductions. The LMRAC's adaptive gains enabled faster settling time and improved disturbance rejection under variable pressure loads (20–120 bar), as evidenced by control signals and reduced output oscillations. While both controllers operated within comparable control voltage ranges (70–260 mV), the LMRAC's nonlinear adaptation laws provided inherent robustness against pump nonlinearities and load sensitivity. These results align with the theoretical predictions from the *Lyapunov* stability analysis, validating the design methodology's effectiveness in addressing the challenges of displacement volume regulation in variable-displacement pumps.

The results obtained from experimental validation of the designed LMRAC and previously designed MRAC and GSAC show that the closed loop system with LMRAC achieves similar control performance as ones for other adaptive control systems. However, the main advantage of LMRAC is that the stability is investigated theoretically.

Future work could explore formal robustness analysis against unmodeled dynamics and integration with predictive load estimation techniques.

Author Contributions: Conceptualization, A.M., T.S. and J.K.; methodology, J.K., A.M. and T.S.; software, J.K.; validation, A.M.; formal analysis, T.S., J.K. and A.M.; investigation, A.M., T.S. and J.K. resources, A.M.; data curation, A.M.; writing—original draft preparation, T.S., A.M. and J.K.; writing—review and editing, J.K. and A.M.; visualization, A.M.; supervision, T.S.; project administration, A.M.; funding acquisition, T.S. All authors have read and agreed to the published version of the manuscript.

Funding: This work has been accomplished with financial support from the European Regional Development Fund within the Operational Programme "Bulgarian national recovery and resilience plan", Procedure for direct provision of grants "Establishing of a network of research higher education institutions in Bulgaria", under the Project BG-RRP-2.004-0005 "Improving the research capacity and quality to achieve international recognition and reSilience of TU-Sofia (IDEAS)".

Data Availability Statement: The original contributions presented in this study are included in the article. Further inquiries can be directed to the corresponding author.

Conflicts of Interest: The authors declare no conflicts of interest.

References

1. Findeisen, D.; Helduser, S. *Ölhydraulik*; Springer: Berlin/Heidelberg, Germany, 2015.
2. Frankenfield, T. Using Industrial Hydraulics. In *Rexroth Worldwide Hydraulics*; Penton Publishing Inc.: New York, NY, USA, 1984.
3. Ivantysyn, J.; Ivantysynova, M. *Hydrostatic Pumps and Motors: Principles, Design, Performance, Modelling, Analysis, Control and Testing*; Academia Books International: New Delhi, India, 2001.
4. Manring, N. *Fluid Power Pumps and Motors: Analysis, Design, and Control*; McGraw-Hill Education: New York, NY, USA, 2013.
5. Kordak, R. Hydrostatic Drives with Control of the Secondary Unit. In *The Hydraulic Trainer Vol.6*; Mannesmann Rexroth GmbH: Lohr a. Main, Germany, 1996; Volume 6.
6. Tonyan, M. *Electronically Controlled Proportional Valves*; Marcel Dekker Inc.: New York, NY, USA, 1985.
7. Sun, Z.; Khalil, M.K.B.; Yurkevich, V.D.; Svoboda, J.; Bhat, R.B. Implementation of single feedback control loop for constant power regulated swash plate axial-piston pumps. *Int. J. Fluid Power* **2002**, *3*, 27–36.
8. Zeng, Q.; Wan, L.; Xiao, Y. Dynamic Response Analysis of the Bi-Tandem Axial-piston Pump with Dual-Loop Positive Flow Control under Pressure Disturbance. *Actuators* **2023**, *12*, 260.
9. Feng, Y.; Jian, Z.; Li, J.; Tao, Z.; Wang, Y.; Xue, J. Advanced Control Systems for Axial-piston Pumps Enhancing Variable Mechanisms and Robust Piston Positioning. *Appl. Sci.* **2023**, *13*, 9658. [CrossRef]

10. Petkov, P.; Slavov, T.S.; Kralev, J. *Design of Embedded Robust Control Systems Using MATLAB®/Simulink®*; IET Control: London, UK, 2018.
11. Mitov, A.; Kralev, J.; Slavov, T.S.; Angelov, I. Design of Embedded Control System for Open Circuit Axial-piston Pump. In Proceedings of the 2022 22nd International Symposium on Electrical Apparatus and Technologies (SIELA), Bourgas, Bulgaria, 1–4 June 2022.
12. Skarpetis, M.G. *Automatic Control of Hydraulic Systems*; Nova Science Publishers Inc.: Hauppauge, NY, USA, 2023.
13. Haggag, S.A. Robust control and modelling of a heavy equipment variable-displacement pump hydraulic system. *Int. J. Heavy Veh. Syst.* **2011**, *18*, 288–302. [CrossRef]
14. Park, S.; Lee, J.; Kim, J. Robust control of the pressure in a control-cylinder with direct drive valve for the variable-displacement axial-piston pump. *Proc. Inst. Mech. Eng. Part I J. Syst. Control Eng.* **2009**, *223*, 455–465. [CrossRef]
15. Zeiger, G.; Akers, A. *The Application of Linear Optimal Control Techniques to Axial-piston Pump Controller Design*; SAE Technical Papers; SAE International: Warrendale, PA, USA, 1989.
16. Lin, S.; Akers, A. Optimal control theory applied to pressure-controlled axial-piston pump design. *J. Dyn. Syst. Meas. Control Trans. ASME* **1990**, *112*, 475–481. [CrossRef]
17. Berg, H.; Ivantysynova, M. Design and testing of a robust linear controller for secondary controlled hydraulic drive. *Proc. Inst. Mech. Eng. Part I J. Syst. Control Eng.* **1999**, *213*, 375–385. [CrossRef]
18. Zeiger, G.; Akers, A. Dynamic Analysis of an Axial-piston Pump Swashplate Control. *Proc. Inst. Mech. Eng. Part I J. Syst. Control Eng.* **1986**, *200*, 49–58. [CrossRef]
19. Berg, H.; Ivantysynova, M. Robust closed loop speed and angular position control for variable-displacement hydraulic motors supplied from a constant pressure mains system. *Olhydraulik Und Pneum.* **1999**, *43*, 405–410.
20. Zhang, R.; Alleyne, A.; Prasetiawan, E. Modeling and H_2/H_∞ MIMO control of an earthmoving vehicle powertrain. *J. Dyn. Syst. Meas. Control Trans. ASME* **2002**, *124*, 625–636. [CrossRef]
21. Lennevi, J.; Palmberg, J.-O. Application and implementation of LQ design method for the velocity control of hydrostatic transmissions. *Proc. Inst. Mech. Eng. Part I J. Syst. Control Eng.* **1995**, *209*, 255–268. [CrossRef]
22. Heybroek, K.; Larsson, J.; Palmberg, J.-O. Open Circuit Solution for Pump Controlled Actuators. In Proceedings of the 4th FPNI-PhD Symposium, Sarasota, FL, USA, 13–17 June 2006; pp. 27–40.
23. Zhang, P.; Li, Y. Research on Control Methods for the Pressure Continuous Regulation Electro-hydraulic Proportional Axial-piston Pump of an Aircraft Hydraulic System. *Appl. Sci.* **2019**, *9*, 1376. [CrossRef]
24. Kemmetmüller, W.; Fuchshumer, F.; Kugi, A. Nonlinear pressure control of self-supplied variable-displacement axial-piston pumps. *Control Eng. Pract.* **2010**, *18*, 84–93. [CrossRef]
25. Wei, J.; Guo, K.; Fang, J.; Tian, Q. Nonlinear supply pressure control for a variable-displacement axial-piston pump. *Proc. Inst. Mech. Eng. Part I J. Syst. Control Eng.* **2015**, *229*, 614–624. [CrossRef]
26. Mitov, A.; Slavov, T.; Kralev, J. Comparison of Advanced Multivariable Control Techniques for Axial-Piston Pump. *Processes* **2024**, *12*, 1797. [CrossRef]
27. Landau, Y.D. *Adaptive Control: The Model Reference Approach*; CRC Press: Boca Raton, FL, USA, 1979.
28. Åström, K.J. *Adaptive Control in Mathematical System Theory: The Influence of RE Kalman*; Springer: Berlin/Heidelberg, Germany, 1995.
29. Helian, B.; Mustalahti, P.; Mattila, J.; Chen, Z.; Yao, B. Adaptive robust pressure control of variable-displacement axial-piston pumps with a modified reduced-order dynamic model. *Mechatronics* **2022**, *87*, 102879. [CrossRef]
30. Han, L.; Wang, H.J.; Li, D.Y.; Yao, Y. MRAC for Direct Drive Electronic-Hydraulic Servo System. *Adv. Mater. Res.* **2012**, *433–440*, 4142–4148. [CrossRef]
31. Plummer, A.R.; Vaughan, N.D. Robust adaptive control for hydraulic servosystems. *J. Dyn. Syst. Meas. Control.* **1996**, *118*, 237–244. [CrossRef]
32. Wei, X.; Wang, L.; Ni, X. Speed control strategy for pump-motor hydraulic transmission subsystem in hydro-mechanical continuously variable transmission. *J. Mech. Sci. Technol.* **2021**, *35*, 5665–5679. [CrossRef]
33. Strano, S.; Terzo, M. Non-Linear Model Reference Adaptive Control of a Hydraulic Actuator in Presence of Parametric Uncertainty. In Proceedings of the RAAD 2012: 21th International Workshop on Robotics in Alpe-Adria-Danube Region, Naples, Italy, 10–13 September 2012; ESA: Paris, France, 2012.
34. Edge, K.A.; Hu, F. Constant pressure control of a piston pump using a model reference adaptive control scheme. In Proceedings of the 11th Aachen Colloquium on Fluid Power Technology, Aachen, Germany, 8–10 March 1994.
35. Busquets, E.; Ivantysynova, M.; Handroos, H. Discontinuous projection-based adaptive robust control for displacement-controlled actuators. *J. Dyn. Syst. Meas. Control Trans. ASME* **2015**, *137*, 8. [CrossRef]
36. Guo, K.; Wei, J. Adaptive robust control of variable-displacement pumps. In Proceedings of the American Control Conference, Washington, DC, USA, 17–19 June 2013.

37. Koivumäki, J.; Mattila, J. Adaptive and nonlinear control of discharge pressure for variable-displacement axial-piston pumps. *J. Dyn. Syst. Meas. Control Trans. ASME* **2017**, *139*, 10. [CrossRef]
38. Rexroth Bosch Group. *Pressure and Flow Control System*; Technical Data Sheet, RE 30630; Rexroth Bosch Group: Lohr am Main, Germany, 2015.
39. Rexroth Bosch Group. *Proportional Directional Valves, Direct Operated, with Electrical Position Feedback as Pilot Control Valve for Control Systems SY(H)DFE*; Technical Data Sheet, RE 29016; Rexroth Bosch Group: Lohr am Main, Germany, 2019.
40. Mitov, A.; Slavov, T.; Kralev, J. Rapid Prototyping of H_∞ Algorithm for Real-Time Displacement Volume Control of Axial-piston Pumps. *Algorithms* **2023**, *16*, 120. [CrossRef]
41. Slotine, J.; Li, W. *Applied Nonlinear Control*; Prentice Hall: Englewood Cliffs, NJ, USA, 1991.
42. Mitov, A.; Slavov, T.; Kralev, J.; Angelov, I. Model reference adaptive control of axial-piston pump. *IOP Conf. Ser. Earth Environ. Sci.* **2025**, *1532*, 012016. [CrossRef]
43. Mitov, A.; Slavov, T.; Kralev, J. Real-Time Gain Scheduling Controller for Axial-piston Pump Based on LPV Model. *Actuators* **2025**, *14*, 421. [CrossRef]
44. Danfoss. *Plus+1 Controllers MC012-020 and 022*; Data Sheet, 11077167, Rev DA; Danfoss: Nordborg, Denmark, 2013.

Disclaimer/Publisher's Note: The statements, opinions and data contained in all publications are solely those of the individual author(s) and contributor(s) and not of MDPI and/or the editor(s). MDPI and/or the editor(s) disclaim responsibility for any injury to people or property resulting from any ideas, methods, instructions or products referred to in the content.